Direct photoinduced surface relief formation in carbazole-based azopolymer using polarization holographic recording

A. MESHALKIN[a*], S. ROBU[a,b], E. ACHIMOVA[a], A. PRISACAR[a], D. SHEPEL[c], V. ABASKIN[a], G.TRIDUH[a]
[a]*Institute of Applied Physics, Academy of Sciences of Moldova, Chisinau, Moldova*
[b]*State University of Moldova, Chisinau, Moldova*
[c]*Institute of Chemistry, Academy of Sciences of Moldova, Chisinau, Moldova*

New carbazole-based azopolymer was synthesized, characterized and applied for formation of photoinduced surface relief gratings. The surface modulation of spin-coated azopolymer film depending on the different polarization configurations is considered. It is shown that holographic surface relief gratings with relatively large thickness modulation could be obtained by direct one-step holographic recording without any subsequent processing steps. Right and left orthogonal circular polarization configuration is the best case, which allows to achieve surface relief grating with the largest amplitude up to 50% of original film thickness. Diffraction efficiency of aluminized grating close to 20% at λ=650nm was obtained.

(Received August 14, 2015; accepted September 29, 2016)

Keywords: Azopolymer, Carbazole, Surface relief grating, Polarization holographic recording

1. Introduction

Electronic and optoelectronic devices using organic materials as active elements have received a great deal of attention from the standpoint of potential technological applications as well as fundamental science. Carbazole-containing polymers have been the subject of intensive investigation since the discovery of its photoconductivity by Hoegl [1]. In addition, these media owing to photorefractive, photoconductive, and photochemical properties [2, 3] are interesting for holographic recording and surface relief formation. The photo-induced features and application of these polymers as recording media were extensively studied by Andries and his group [4-6].

The commercial availability and relative cheapness of the starting materials, simple synthetic method and a number of sites available for easy functionalization, good charge drift mobility and solubility in common organic solvents makes the carbazole-containing polymers attractive building blocks for the construction of more complex materials for optoelectronic applications.

The most commonly used method to form diffraction gratings is holographic recording with which a sinusoidal modulated intensity pattern can be obtained at the submicron scale. It was shown in [7] that holographic gratings could be obtained on carbazole materials that are involved an exposure of the thin film to an interference pattern. Direct fabrication of surface relief gratings by laser interference lithography was shown in [8].

In recording media, carbazole-based polymer included, during the holographic recording two coupling gratings are formed simultaneously: 1 - phase grating, due to modulation of the refractive index and/or thickness of materials, and 2 - amplitude grating, resulting from the changes of absorption coefficient. To enhance the diffraction efficiency of the gratings the surface relief structuring is developed by wet or dry etching. However, these chemical processes, especially wet etching based on solvent dissolutions, complicate the technological process (deform the surface structures, increase the background scattering), and make it less promising for practical application.

Recently, new organic materials named azobenzene-containing polymers (azopolymers) have attracted much attention for the fabrication of surface structures [9-11]. Both scalar and polarization holographic recordings have been employed to generate surface relief structures in many azobenzene-containing materials, including monomers and polymers [12-14]. The phase modulating materials can produce a higher efficiency than an amplitude modulating material. In the phase modulating materials, there is no absorption of light and the entire incident light is available for image formation, while the incident light is significantly absorbed in an amplitude modulating material.

Kim's group first showed a new possibility to direct formation of surface relief gratings (SRG) on azopolymer films without any subsequent processing steps due to mass transport effect under a modulated light irradiation [15]. It was reported that large surface modulations by a simple one-step process can be obtained on azopolymer films.

Many theoretical models were proposed to explain the process of SRG formation, but the mechanism is still not fully explained [16-19]. In any case, the important role is played by the creation of dipole moment under photoexcitation. The dipoles are able to acquire selective orientation reacting to the direction of the electric vector of the light wave. The widely used model is the gradient

force model [20]. According to this model, the resultant force can be achieved due to the light irradiation, which induces a trans-form ↔ cis-form photoisomerization effect in azobenzene molecules. In addition, it was found [21] that type of polymer matrix and molecular weight was a crucial parameter in SRG formation.

Up to our knowledge, there are not papers regarding to azo-dyed carbazole-based polymer films, where surface relief gratings were recorded by polarization holography. In this work we synthesized and characterized of new carbazole-based azopolymer suitable for direct surface relief grating formation, and performed the surface modulation of prepared films in dependence on the polarization states of recording beams.

2. Materials and methods

Azopolymer synthesis

Carbazole-based monomer N-epoxypropylcarbazole (EPC) and azodye Disperse Orange (DO) was utilized in this study. Disperse Orange 3 (4-(4-nitrophenylazo)aniline) with dye content 90% and molecular weight 242 was purchased as a commercial product from Sigma-Aldrich Company. DO molecule was chemically attached to EPC monomer by polycondensation scheme at a temperature of 120º C for 4 hours. The molar ratio between EPC and DO was 90/10. The obtained azopolymer was purified by precipitation in hexane and then in methanol. Chemical structure of EPC:DO (90:10) is presented in Fig. 1.

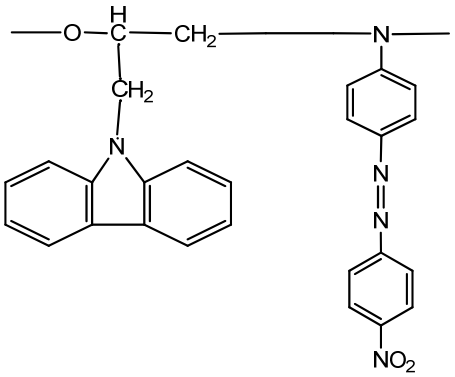

Fig. 1. Chemical structure of synthesized azopolymer EPC:DO (90:10).

Fourier Transform Infrared Spectroscopy (FTIR) was applied for copolymer structure characterizing and identifying organic molecules [22]. FTIR is an essential and crucial characterization technique to elucidate the structure of matter at the molecular scale. The chemical composition and the bonding arrangement of constituents of the monomer, the azodye, and the azopolymer were investigated by FTIR spectroscopy. The IR spectrum represents the molecular absorption and transmission, creating a molecular fingerprint of the sample. Position of absorption peaks correspond to the frequencies of vibrations between the bonds of the atoms and the size of the peaks is a direct indication of the amount of constituents. Before infrared analysis, powdered samples were dried in exsiccator up to constant mass. Infrared spectra of the samples were recorded with a PerkinElmer Spectrum 100 FT-IR spectrometer. Data collection covers a total spectral range from 7800 cm^{-1} to 400 cm^{-1} with the resolution 4 cm^{-1}.

Formation of polymer films from solution

A widely used technique to produce thin layers is spin-coating. In spin-coating, a solution drop of the coating material dissolved in an appropriate solvent is dispensed onto the substrate surface, which is made to rotate at large velocity (typically around 600 – 3000 rpm). The spinning motion spreads out the solution and, as the solvent evaporates away, a thin film of coating is left on the surface. There are several major factors affecting the coating process. Among these are spin speed, acceleration, spin time and exhaust volatility. It was shown that spin coating of thin and thick polymer films, examined in several solvents of varying volatility over a broad range of polymer solution concentrations and spin speeds, could give film thicknesses from 10 nm to 33 pm [23].

In our study the thin polymer films were prepared from the 10wt. % homogeneous polymer solution in toluene onto glass substrate using programmable spin-coater "SGS Spincoat G3P-8". Operation conditions for polymer solution deposited on 5 cm diameter optical glass substrate (BK7) were as follows: 1 cm^2 of liquid dispensed on the disk at rest, subsequently accelerated in about 3 s to 800 rpm and spun for 60 s. Obtained films were dried in a oven at 60°C for 6 hours.

Determination of film thickness

For the determination of film thickness the modified digital MII-4 interference microscope with CCD-camera was applied [24, 25]. A magnification of 490^x was used. The area, from which a data analysis is performed, was 0.3 mm diameter circle. The interference pattern of light reflected from a flat reference surface and the surface of investigated sample was recorded in PC. The software tool OpticMeter has been elaborated for PC processing of interferograms. It permits to fit the interference patterns in an analytical form and precisely calculate the lines shift corresponding to thickness of submicrometer films. This enables a height resolution better than 15 nm. The thickness of films determined from the fringe pattern in the interferograms was about 270 nm.

Spectral characterization

UV-VIS transmission spectra were recorded on thin polymer films with Specord M40. Good optical quality films were obtained after a drying period of 6 hrs.

Holographic characterization

The experimental setup based on DPSS laser (532 nm, 100 mW) used for holographic recording was described in [26] and shown in Fig. 2.

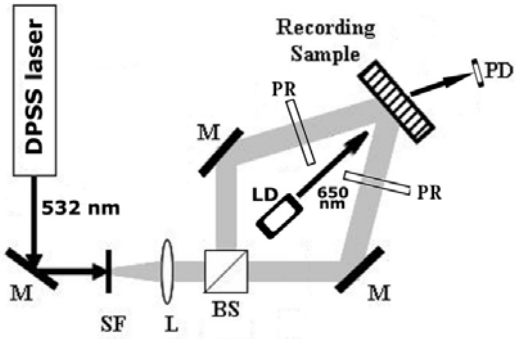

Fig. 2 Optical arrangement for holographic grating recording with real-time measurement of diffraction efficiency by photodetector. CW DPSS laser (λ=532 nm, power =100 mW), M – mirror; SF – spatial filter; L – collimating lens; BS – beam splitter; LD – laser diode (λ = 650 nm) for monitoring recording process; PR- wave plate; PD – photodetector.

The laser beam was split into two identical beams by a 50/50 non-polarized beam splitter so the intensity balance between two interfering beams was near 1:1. The two beams were then combined, by using two mirrors, and interfered on the azopolymer film surface. The polarization states of the two laser beams were controlled independently by quarter or half wave plates. The incident angle was adjusted by tuning the two mirrors symmetrically respect to the sample surface, and grating period was 1 μm. The intensity of interference beams was varied at the sample surface from 160 mW/cm^2 up to 270 mW/cm^2. In order to monitor the kinetics of grating formation, a probe red beam of laser diode (LD) (λ = 650 nm, power = 1 mW/cm^2) was sent into the interference area, and the first-order diffraction intensity (η) was measured as a function of time. A detection system consisted of a photodiode placed behind the sample, an amplifier and an A/D converter with 12-bit resolution, to detect and record first-order diffraction intensity of the probe beam on PC during grating recording.

In this work, a number of gratings were experimentally realized and polarization states influence on the SRG formation was investigated. In this work we examined three polarization configurations:

1. S:S parallel vertical linear polarizations (perpendicular to direction of grating vector);
2. +45º:-45º orthogonal linear polarizations with the polarization planes oriented at an angle of 45º with respect to a grating vector direction;
3. RC:LC right and left orthogonal circular polarizations.

Our choice of these configurations is determined by following considerations. The two parallel linear (S:S or P:P) polarized beams produce the largest light intensity modulation. There is no spatial modulation in the direction of the resultant electric vector of light. Under the polarization modulated holographic recording, the two orthogonal linear (S:P and +45^o:-45^o) and circular (RC:LC) polarized beams produce the largest variation in the resultant electric field direction on the film surface but the light intensity is uniform over the entire exposed area. It was shown in [27] that polarization recording configurations S:S, S:P and P:P produce very small surface modulation but orthogonal linear (+45^0:-45^0) and circular (RC:LC) polarization configurations provide the largest surface relief modulation. In order to evaluate intensity modulation of the two-beam interference pattern for different polarization configurations we used parameter called interference contrast K given by expression $K = \left|\frac{I_{\max} - I_{\min}}{I_{\max} + I_{\min}}\right| * 100\%$, where I_{max} and I_{min} are the maximum and minimum of the light intensity in the interference pattern. The interference intensity distribution was calculated for grating period Λ=1μm corresponding to angle between incident beams Θ=30.85^o at λ=532nm. The theoretical calculation of resulted light intensity modulation, polarization distribution and interference contrast of the two-beam interference pattern with Λ=1μm for S:S, +45^o:-45^o and RC:LC polarization configurations are presented in Fig. 3.

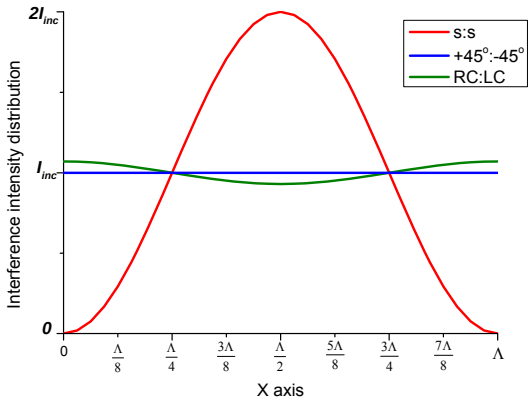

Fig. 3. Theoretical calculation of the light intensity modulation and polarization distribution of the two-beam interference pattern for S:S, +45^o:-45^o and RC:LC polarization configurations. Here Iinc is a sum of light intensities of the incident interfering beams.

The contrast of interference pattern (K) at the sample surface during holographic recording was calculated according to [28]. The interference contrast was calculated for grating period Λ=1μm corresponding to angle between incident beams Θ=30.85^o at λ=532nm. The resulted polarization distributions and the contrasts in the interference pattern are presented in Table 1.

Therefore, the interference pattern with S:S polarization configuration and interference contrast K=100% ensures best intensity modulation contrast and interference polarization keeps the same direction. Contrary to it, +45^o:-45^o polarization configuration has no intensity modulation, but interference resulted polarization

varies periodically between linear, elliptical and circular forms. For the case of RC:LC polarization configuration, the resultant polarization becomes a linear polarization where the polarization direction changes periodically, and there is 7% of interference pattern contrast .

Table 1. The resulted polarization distribution and contrast K of the interference pattern for different polarization configurations.

Polarization of recording beams	Resulting electric field vector pattern (*x-y* plane)					Contrast of interf. pattern
x:	+Λ/2	+Λ/4	0	-Λ/4	–Λ/2	κ %
S:S	•	↕	↕	↕	•	100
+45°:-45°	↔	○	↕	○	↔	0
RC:LC	↔	↗↙	↕	↘↖	↔	7

Surface relief measurements

After recording an atomic-force microscopy (AFM NANOStation II) was applied for relief formation investigations. It was studied the variation of relief height with polarization configuration.

3. Results and discussion

The constituents of synthesizing copolymer (monomer EPC, azo-dye DO) and copolymer EPC:DO obtained were characterized by FTIR spectroscopy with attribution of infrared absorption bands to main functional groups. On the Fig. 4 we present IR spectrum of the monomer EPC and the copolymer EPC:DO. The conjunction of azo group in synthesized copolymer EPC:DO was confirmed by the appearance of the peak at 1389 cm^{-1} in the IR spectrum (Fig. 4) corresponding to the N = N stretching frequency [29].

The synthesized azopolymer EPC:DO was soluble in common organic solvents, namely toluene, and formed good optical quality films by spin coating which proved by UV–Visible–NIR transmittance spectrum of the thin films (the thickness 270 nm) of monomer EPC and copolymer EPC:DO shown at Fig 5, because in the interference maxima transmission is near the transmission of glass substrate.

From comparison of these spectra one can see the absorption band on EPC:DO spectra ranges from 350 nm to 580 nm with an absorption peak at 460 nm.

The spectra are displayed the influence of azo-dye component (DO) on the general transmission spectra of EPC monomer. The transmittance value for EPC:DO is 59% at green light against 87% for EPC. Therefore the wavelength of 532 nm is suitable for the SRG formation. Nonactinic LD wavelength of 650 nm which is out of the absorption band of the DO molecules was used for monitoring recording process.

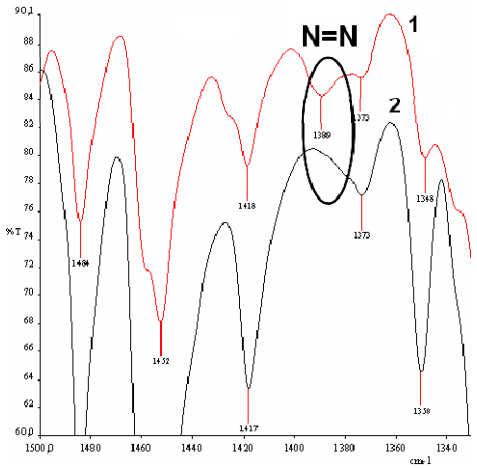

Fig. 4. Fragments of IR spectrum: 1- copolymer EPC:DO (90:10); 2 – EPC

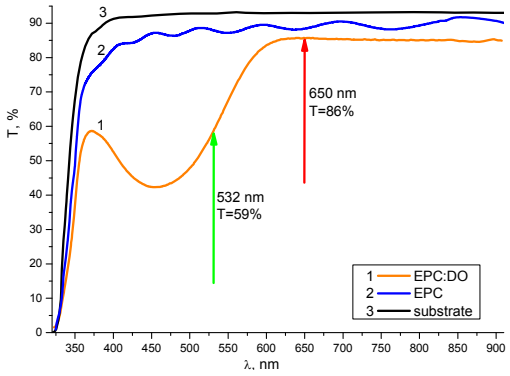

Fig. 5. Transmittance spectra of thin films of the EPC:DO copolymer, the EPC monomer and glass substrate.The arrows indicate the position and transmission at the wavelength 532 nm and 650 nm. The thickness of film was about 270 nm.

At Fig. 6 the time dependence of the first-order diffraction efficiency of recorded gratings are shown using different polarization configurations.

As it is seen from Fig.6 the S:S polarization configuration, providing the best intensity modulation in exposed area, doesn't lead to grating formation. But in the case of +45º:-45º and RC:LC polarization configuration, which does not create intensity modulation or at least the small amount of it (K=7% for RC:LC), allows to obtain surface gratings with high diffraction efficiency.

So the formation of grating on azopolymer therefore depends strongly on the polarization distribution. The value of diffraction efficiency is specified by the refractive index difference between recording media and air that consist about 0.5. It was shown in [30] that thin metal coatings could strongly enhance diffraction efficiency of surface relief gratings. In our experiment aluminum (Al) metal coating by thermal vacuum evaporation allowed to increase of diffraction efficiency of SRG (in reflection

mode) recorded by RC:LC polarization configuration close to 20%. Moreover it was shown that thermal vacuum evaporation of Al didn't deform the surface grating obtained by holographic recording.

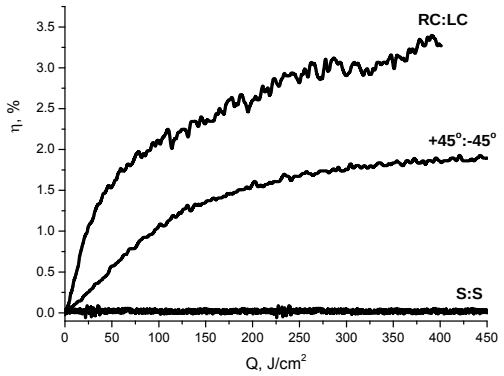

Fig. 6. Dose dependences on the first-order diffraction intensity measured at 650 nm in transmission mode during recording by 532nm laser at 3 polarization states.

From Fig. 6 it is seen that not only the maximal shown diffraction efficiency, but the kinetics of grating recording process depends on the state of polarization of the recording beams. For RC:LC and +45º:-45º polarization configurations we observed the constant rise of η but with a different rate. At doze of 100 J/cm^2 the diffraction efficiency reaches 1% for +45º:-45º against 2% for RC:LC state of polarization.

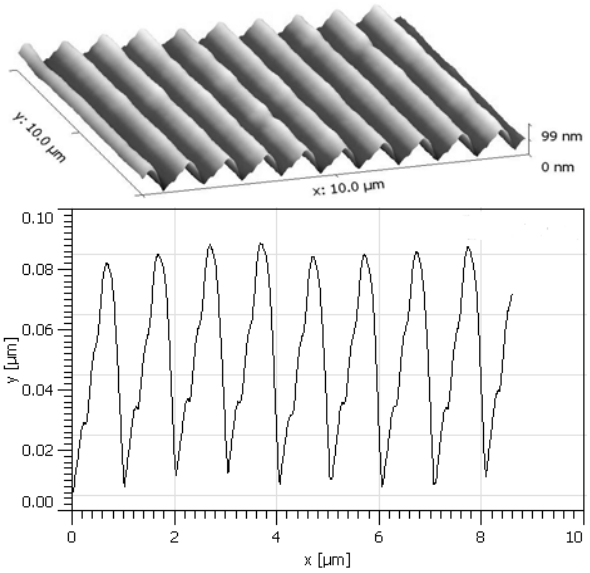

Fig. 7. Three-dimensional view and profile of surface gratings recorded under +45º:-45º polarization configuration.

The surface of the gratings on polymer films was investigated ex situ by atomic force microscopy (AFM). In the Fig. 7 and Fig. 8 the AFM three-dimensional view and profile of surface gratings recorded under +45º:-45º and RC:LC polarization configurations are shown respectively.

AFM measurements showed very regularly spaced surface relief structures with a period of 1µm. In case of +45º:-45º polarization configuration the depth of the surface relief patterns was about 80 nm which is approximately 30% of the original film thickness (270 nm).

In case of RC:LC polarization configuration the depth of the surface relief patterns was about 130 nm which is approximately 48% of the original film thickness.

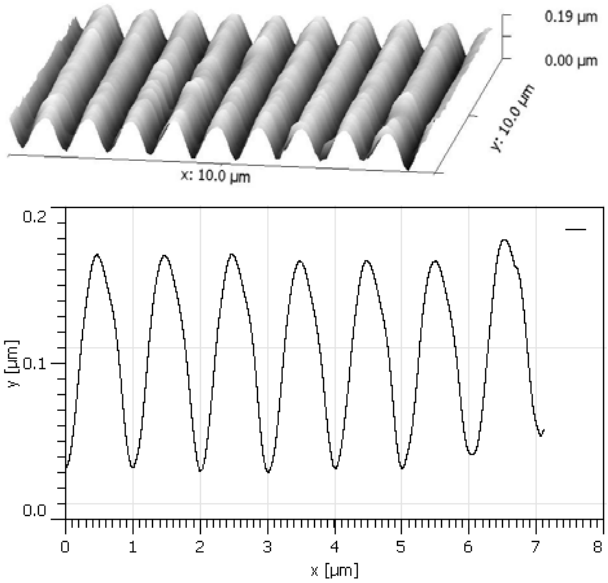

Fig. 8. Three-dimensional view and profile of surface gratings recorded under RC:LC polarization configuration.

At the Fig. 9 the three-dimensional view and profile of surface gratings recorded under RC:LC polarization configuration after Al metallization are shown. As it is seen the relief structures wasn't destroyed by thermal evaporation of Al and the height of grating remained the same value of 130 nm.

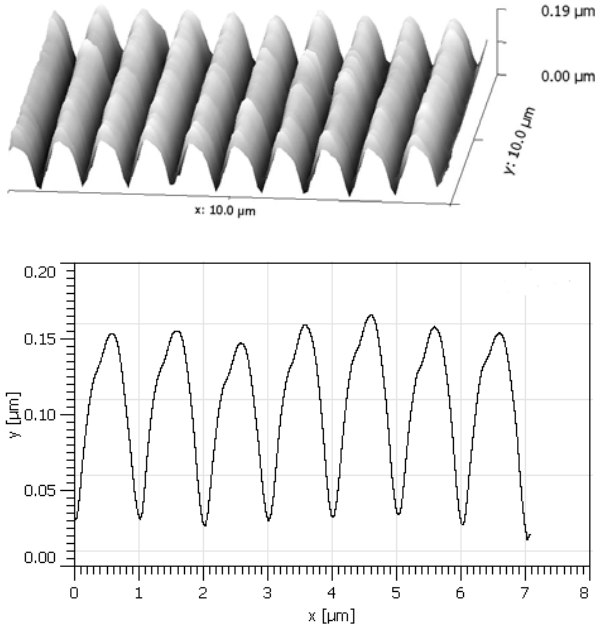

Fig. 9. Three-dimensional view and profile of surface gratings recorded under RC:LC polarization configuration after Al metallization of grating surface.

4. Conclusions

We report the observation of direct one-step holographic surface relief gratings recording on azolymer EPC:DO.

We found that the RC:LC polarization configuration is the best case among the studied polarizations, which allows to achieve surface relief grating with the largest amplitude about 130nm (48% of film thickness). Diffraction efficiency in reflection mode of aluminized SRG recorded by RC:LC polarization configuration was close to 20%.

On the other hand, the S:S polarization configuration, providing only the intensity modulation, didn't lead to grating formation.

The formation of surface relief grating therefore depends strongly on the polarization state combinations of recording beams.

Acknowledgments

The authors thank Mihail Enaki and the National Center for Materials Study and Testing (Technical University of Moldova) for performing AFM measurements.

The research was partially supported by the project HOLO-H2020-TWINN-2015 No 687328 and Institutional Project CSSDT 15.817.02.04A.

References

[1] H. Hoegl, J. Phys. Chem. **69**(3), 755 (1965).
[2] J. V. Grazulevicius, P. Strohriegl, J. Pielichowski, K. Pielichowski, Prog. Polym. Sci. **28**(9), 1297 (2003).
[3] B. Mailhot-Jensen, S. Robu, A. Rivaton, J. Pilichowski, A. Chirita, E. Chilat, G. Dragalina, Int. J. Photoenergy **2010**, ID945242 (2010).
[4] A. Andriesh, V. Bivol, A. Prisacar, S. Sergheev, A. Meshalkin, S. Robu, N. Barba, N. Sirbu, J. Optoelectron. Adv. M. **7**(3), 1169 (2005).
[5] Andries, V. Abaskin, E. Achimova, A. Meshalkin, A. Prisacar, S. Sergheev, S. Robu, L. Vlad, Phys. Status Solidi A **208**(8), 1837 (2011).
[6] A. Andriesh, M. Iovu, Phys. Status Solidi B **246**(8), 1862 (2009).
[7] A. Andriesh, S. Sergheev, G. Triduh, A. Meshalkin, J. Optoelectron. Adv. M. **9**(10), 3007 (2007).
[8] M. Vlcek, S. Schroeter, S. Brueckner, S. Fehling, A. Fiserova, J. Mater. Sci: Mater. Electron. **20**, S290 (2009).
[9] V. M. Kryshenik, M. L. Trunov, V. P. Ivanitsky, J. Optoelectron. Adv. M. **9(7)**, 1949 (2007).
[10] M. Watabe, G. Juman, K. Miyamoto, T. Omatsu, Sci. Rep. **4**, 4281 (2014).
[11] T. Seki: in Smart Light-Responsive Materials, ed. Y. Zhao and T. Ikeda (Willey, Hoboken, NJ, 2009) p. 273.
[12] N. K. Viswanathan, S. Balasubramanian, L. Li, S. K. Tripathy, J. Kumar, Jpn. J. Appl. Phys. **38**, 5928 (1999).
[13] L. Nikolova, T. Todorov, M. Ivanov, F. Andruzzi, S. Hvilsted, P. S. Ramanujam, Appl. Opt. **35**(20), 3835 (1996).
[14] R Barille, P. Tajalli, S. Zielinska, E. Ortyl, S. Kucharski, J. M. Nunzi, Appl. Phys. Lett. **95**(5), 053102 (2009).
[15] D. Y. Kim, S. K. Tripathy, L. Li, J. Kumar, Appl. Phys. Lett. **66**, 1166 (1995).
[16] D. Bublitz, B. Fleck, L. Wenke, Appl. Phys. B **72**, 931 (2001).
[17] B. Bellini, J. Ackermann, H. Klein, Ch. Grave, Ph. Dumas, V. Safarov, J. Phys. Condens. Matter. **18**, S1817 (2006).
[18] M. L. Juan, J. Plain, R. Bachelot, P. Royer, S. K. Gray, G. P. Wiederrecht, ACS Nano **3**(6), 1573 (2009).
[19] S. Lee, H. S. Kang, J. K. Park, Adv. Mater. **24**(16), 2069 (2012).
[20] J. Kumar, L. Li, X. L. Jiang, D. Y. Kim, T. S. Lee, S. K. Tripathy, Appl. Phys. Lett. **72**(17), 2096 (1998).
[21] K.G. Yager, C. J. Barrett, Curr. Opin. Solid State Mater. Sci. **5**, 487 (2001).
[22] N. Eidelman, C. G. Simon, J. Res. Natl. Inst. Stand. Technol. **109**, 219 (2004).
[23] D. Hall, P. Underhill, J. Torkelso, Polym. Eng. Sci. **38**(12), 2039 (1998).
[24] A. Meshalkin, V. Abashkin, A. Prisacar, G. Triduh, I. Andries, L. Bets, E. Achimova, Sensor Electronics and Microsystem Technologies **3**(9), 62 (2012).
[25] A. Meshalkin, I. Andriesh, V. Abashkin, A. Prisacar, G. Triduh, E. Achimova, M. Enachi, Surf. Eng. Appl. Elect+ **48**(6), 114 (2012).
[26] E. Achimova, A. Stronski, V. Abaskin, A. Meshalkin, A. Paiuk, A. Prisacar, P. Oleksenko, G. Triduh, Opt. Mater. **47**, 566 (2015).
[27] J. Teteris, U. Gertners, IOP Conf. Series: Materials Science and Engineering **38**, 012012 (2012).
[28] L. Z. Cai, X. L. Yang, Optics&Laser Techn. **34**, 671 (2002).
[29] K. J. Sakoma, K. A. Bello, M. K. Yakubu, Open Journal of Applied Sciences **2**, 54 (2012).
[30] F. Lütolf, M. Stalder, O. Martin, Opt. Lett. **39**(23), 6557 (2014).

*Corresponding author: alexei@asm.md